A RNA-seq replicates

B RNA-seq

pearson 1 0 -1

rods cones HC SAC
1 2 3 1 2 3 1 2 3 1 2 3

SAC HC **cones** cones **rods** rods rods (rd7)

Supplementary figure 1:

(A) Reproducibility of cell isolation as measured by RNA-seq. Correlation heatmap comparing RNA-seq signal for biological replicates. Pearson correlation for genic RNA-seq signal for samples issued from independent cell sorts for each cell type studied.

(B) Comparison of the generated expression profiles with photo-receptors sorted by INTACT nuclei-purification procedure. Correlation heatmap comparing RNA-seq signal obtained in this study using whole cell purification (bold labels) with previously generated nuclear RNA-seq datasets for the same cell types (Mo et al, 2016) (normal labels).
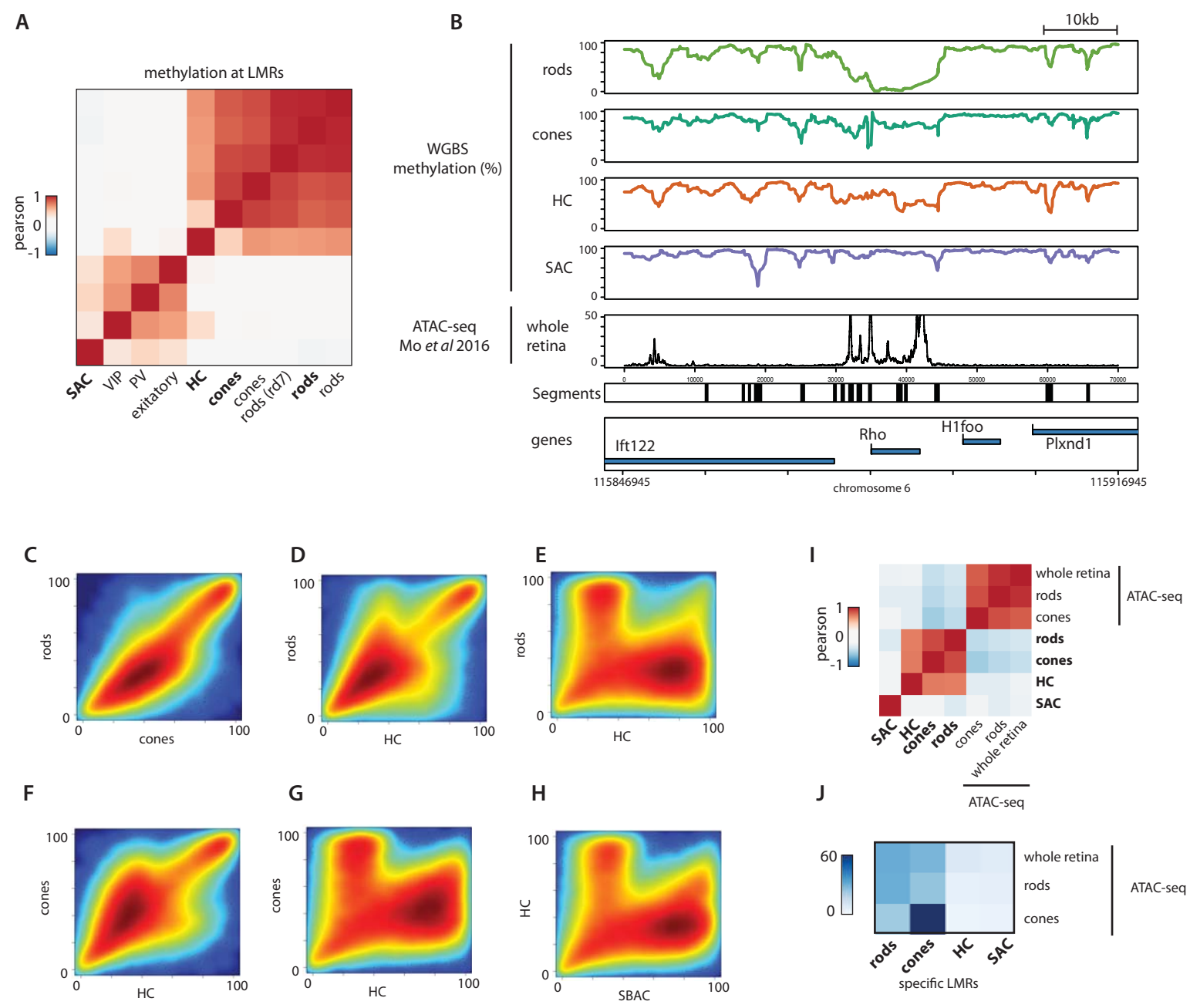
Supplementary figure 2:

(A) Comparison of the generated WGBS data with datasets previously generated by INTACT-nuclei purification procedure. Correlation heatmap comparing single CpG methylation levels at LMRs (bold labels) with previously generated datasets for retinal and neuronal cell types (Mo et al, 2015, 2016) (normal labels).

(B) Rod specific hypo-methylation is observed at the Rhodopsin gene locus. Shown is the average smoothed methylation for the indicted cell types over a 70 kb chromosomal region around the rod specific Rhodopsin gene. Read counts for accessibility measure of total retinas (ATAC-seq) is shown as smoothed signal. Black boxes denote regions having low methylation in at least one of the analyzed cell types, representing putative retinal CREs. (C-H) Variation of DNA methylation levels at LMRs across the four retina cell types. Pairwise smoothed scatter plots representing average methylation levels for LMRs in the corresponding cell types. (I) Quantitative comparison of methylation levels at LMRs with chromatin accessibility as measured by ATAC-seq. Correlation heatmap comparing average methylation levels at LMRs (bold labels) with previously generated ATAC-seq datasets in whole-retina and isolated photoreceptors (Mo et al, 2016) (normal labels). (J) Overlap between cell type-specific LMRs identified in isolated cell types with accessibility in whole-retina and photoreceptors. Heatmap depicting the percentage overlap between LMRs detected in isolated cell types (x axis) and ATAC-seq signal in whole retina or isolated photoreceptors (log2(RPKM)>0.5) (y axis) (Mo et al, 2016).
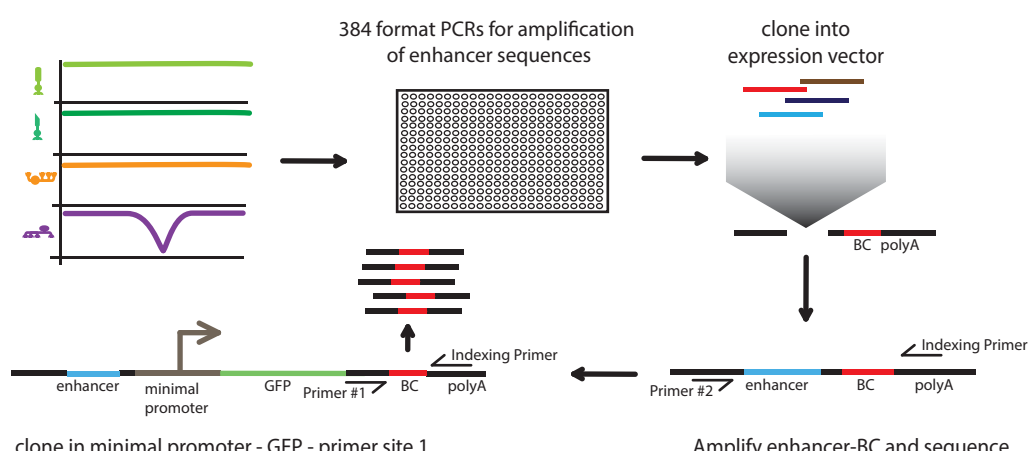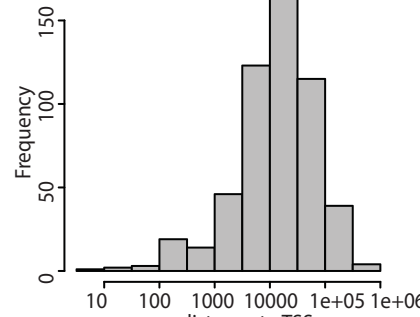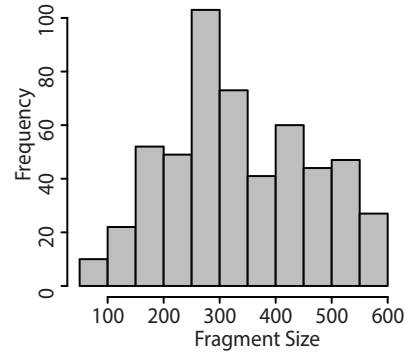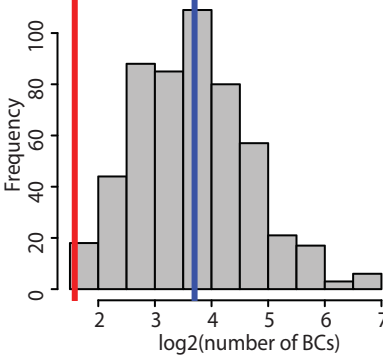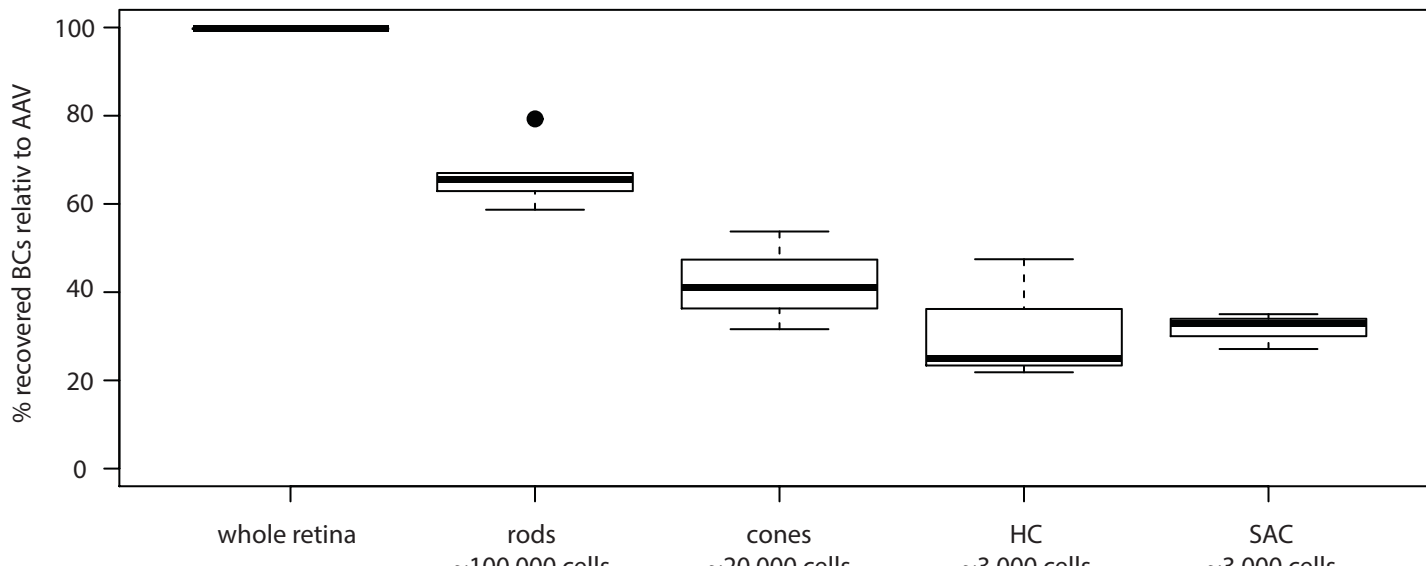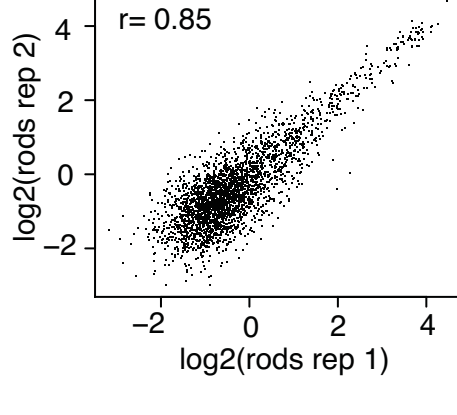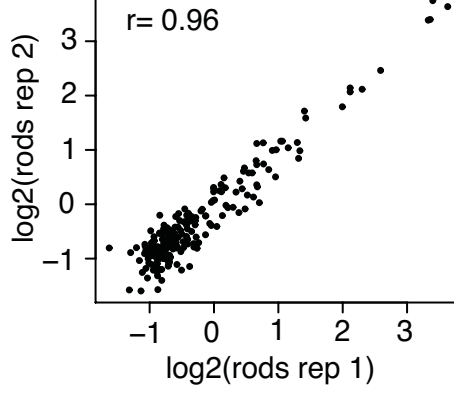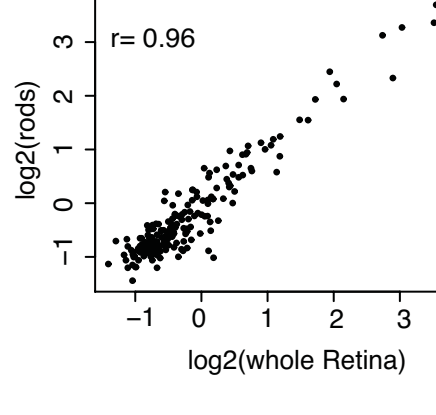
Supplementary figure 3:
(A) Experimental procedure used to construct the PRA libraries.
Methylation maps informed on putative CREs, fragments were PCR amplified in 384-well format and pooled.
Pooled fragments were cloned into a vector containing the expression cassette consisting of a multiple cloning site, a random 15bp barcode sequence and a polyA signaling sequence (pA). In order to average out the contribution of barcode specific biases to the signal we aimed for at least ten different barcodes per unique fragment. To link CREs to barcodes the CRE-barcode sequences were amplified using Primer #2 and one of the Indexing primers (Primers #3-11) containing the Illumina flow cell annealing sequences. PCR products were purified and sequenced. Next the vector was cut between the enhancer and BC and a sequence containing a 31bp minimal promoter, CpG free eGFP and the annealing sequence for Primer #1 was cloned in. Subsequently the construct was cut out of the cloning vector into the AAV vector for virus packaging. (Also see methods)
(B) Most tested putative CREs are located kilobases away from genes. Histogram displaying distance distribution of assayed CREs to nearest transcriptional start site. (C) The tested CREs are restricted in size, not exceeding 600bp. Histogram displaying size distribution of assayed CREs.
(D) Histogram displaying distribution of number of barcodes per CRE. The red line indicates cutoff for minimal number of Barcodes per CRE in the reporter assay (3 BCs), the blue line represents median BCs per CRE (13 BCs).
(E) Fraction of recovered barcodes scales the number of sampled cells and cell number tested. Boxplot displaying percentage of unique barcodes recovered in the different cell types relative to their representation in the AAV input for all cell types tested. Each box shows % recovered barcodes of all replicates for per cell type.
(F) PRA signal reproducibility at the level of barcodes in sorted rod photoreceptors. Reproducibility of barcode level activity is illustrated here by comparing two independent biological replicates.
(G) Using multiple barcodes to derive CRE activity levels enhance PRA accuracy. PRA signal reproducibility at the level of fragment in sorted rod photoreceptors. Activities of multiple barcodes (median ~13) is used to derive mean activity for each tested fragment to reducing the technical noise of the assay.
(H) The tested set of CRE shows very similar activity between rods and whole retina. Scatterplot comparing activity of CREs at the fragment level in whole Retina and rods.

Hartl et al, Supplementary Figure 3
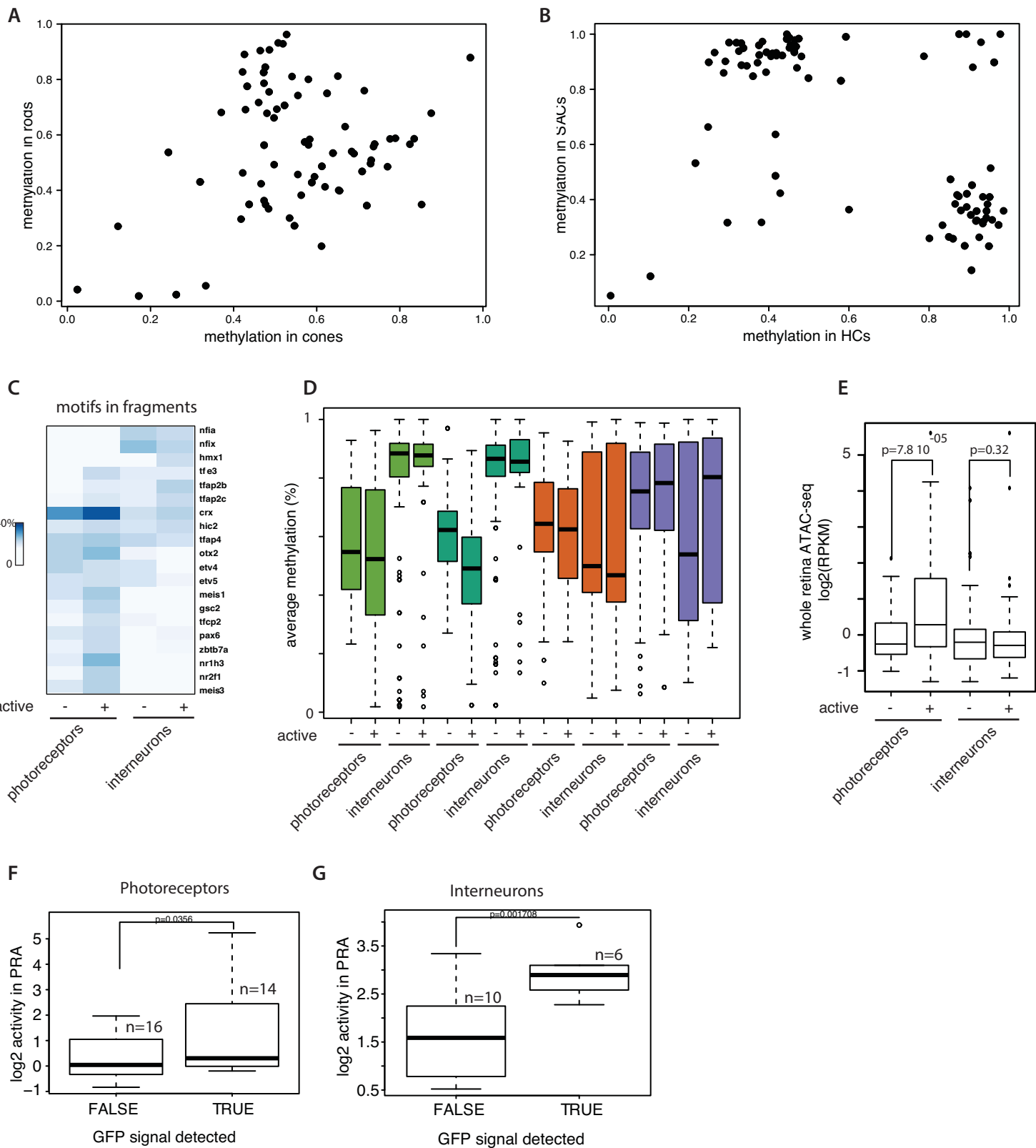
Supplementary figure 4:

(A-B) Scatterplot depicting the average methylation levels of the regions used to design the constructs in (A) library #2 and (B) library #3. Methylation is compared among photoreceptors or interneurons.

(C) Active fragments have slightly more TF binding sites than inactive ones. TF motifs enriched within fragments showing activity in photoreceptors or interneurons. Activity of a fragment was defined by PRA. Shown are motif occurrence frequencies in % for the indicated set of fragments after subtracting motif frequency in a background set of sequences. (D) Methylation levels of endogenous regions from which fragments originate are displayed as a function of their activity in the PRA. (E) Active fragments tend to have higher chromatin accessibility than inactive ones. Same as D but showing chromatin accessibility of endogenous regions relative to their activity in the PRA. ATAC-seq data from whole retina were used (Mo et al, 2016). p-values were derived using a bi-directional t-test.

(F-G) Single fragment validation results are in good agreement with PRA activity measures. Boxplot depicting comparing the PRA measured activity for fragments showing or not detectable Chrd2-GFP in (F) photoreceptors (G) interneurons. The fragments where Chr2-GFP is detected by immunostaining have significantly higher PRA activity in the respective cell type. P-value was calculated using an unidirectional t-test.

A

rorb
nr2e3
nr4a1
rxrg
nr6a1
nr1h3
nr2f1
nr2e1
nr4a2
nr1h4
ppara

rods cones HC SAC
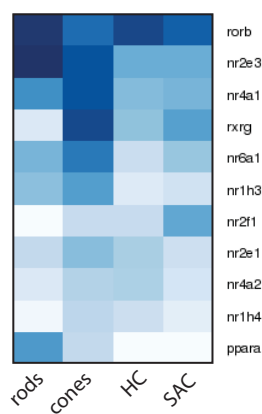
Supplementary figure 5:
(A) Repertoire of nuclear receptors expressed in the studied cell types. Heatmap representing RPKM for nuclear receptors expressed in at least one of the studied cell type. Heatmap was organized by hierarchical clustering.

cell type	mouse strain
rods	b2-Cre x B6.Cg-Gt(ROSA)26Sortm9(CAG-tdTomato)Hze/J # 007913
cones	d4-Cre x B6.Cg-Gt(ROSA)26Sortm9(CAG-tdTomato)Hze/J # 007911
horizontal cells	B6Cf1-Tg(Gja10-Cre, #14)BR x B6.Cg-Gt(ROSA)26Sortm9(CAG-tdTomato)Hze/J # 007917
starburst amacrine cells	129S6-Chat_tm1(cre)Lowl/J x B6.Cg-Gt(ROSA)26Sortm9(CAG-tdTomato)Hze/J # 007921

Supplementary Table 1: Table of mouse strains used to FACS sort specific cell types from the whole retina (Siegert *et al*, 2009).

chromosome	start	end	strand	ID	SACMeans	HCMeans	wholeMeans	rodMeans_lib1	coneMeans_lib2	rodsMeans_lib2	GFP signal detected in	csPRA prediction
chr16	49817994	49818185	-	144-/Intergenic2	0.1448962	0.7817183	4.1180784	3.130001537	3.193095825	2.777570411	Photoreceptors	Photoreceptors
chr17	48473681	48474023	-	217-/Trem2-Intra	NA	NA	NA	0.919568521	NA	NA	Photoreceptors	Photoreceptors
chr18	60942592	60942910	+	218+	0.2246052	0.5558612	0.4719649	0.570810657	0.547496002	-0.502445419	negative	Photoreceptors
chr4	153317537	153317650	+	259+	NA	NA	NA	-0.922875571	0.086656356	-0.962055755	negative	Photoreceptors
chr5	28472582	28472934	-	128-/Intergenic1	NA	NA	NA	2.447912426	1.585804797	1.486156309	Photoreceptors	Photoreceptors
chr7	20015162	20015346	+	262+	NA	NA	NA	-0.834708042	NA	NA	negative	negative
chr9	108433361	108433572	+	108+	NA	NA	NA	-0.234098952	NA	NA	negative	negative
chr9	64799176	64799667	-	112-	1.3081915	0.6281876	5.2348589	NA	NA	NA	Photoreceptors	Photoreceptors
chr9	98892095	98892355	-	107-/Faim-Intra	0.5212305	0.4705372	4.0082861	3.694082443	3.106615399	3.071354462	rods	Photoreceptors
chr10	75067780	75068255	+	524+	NA	NA	NA	NA	0.307958584	-0.642933092	Photoreceptors, HC, Mueller	Photoreceptors
chr10	95018573	95019092	-	283-	NA	NA	NA	NA	-0.195550916	-0.778190793	Photoreceptors	Photoreceptors
chr14	68252390	68252858	+	427+	NA	NA	NA	NA	-0.320660988	-0.740342556	Photoreceptors, Mueller	Photoreceptors
chr1	64399627	64400178	-	483-	NA	NA	NA	NA	0.278933508	-1.073349105	Photoreceptors, Mueller	Photoreceptors
chr3	30669079	30669564	+	360+	NA	NA	NA	NA	0.219970671	-0.8625043	Photoreceptors, Mueller	Photoreceptors
chr3	57348332	57348893	+	506+	NA	NA	NA	NA	-0.012080873	-0.650201155	Photoreceptors, Mueller	Photoreceptors
chr5	53662011	53662512	-	357-	NA	NA	NA	NA	-0.161178677	-0.582074305	Photoreceptors, Mueller	Photoreceptors
chr7	87193812	87194240	-	330-	NA	NA	NA	NA	-0.060127345	-1.13118179	Photoreceptors, Mueller	Photoreceptors
chr8	49596516	49597041	+	359+	NA	NA	NA	NA	0.302115742	-0.739830871	Photoreceptors, ganglion cells	Photoreceptors
chr10	114602962	114603205	-	3274-	0.57325865	2.24826702	-0.342795558	NA	NA	NA	Mueller	Interneurons
chr12	75335993	75336295	+	3285+	3.33951396	2.82205884	1.1984568	NA	NA	NA	negative	Interneurons
chr1	38455370	38455657	-	3192-	2.5687756	2.73769384	0.900204402	NA	NA	NA	Mueller, Glia cells	Interneurons
chr3	131727036	131727461	+	3010+	1.65020139	0.56919204	-0.658386556	NA	NA	NA	ganglion cells	negative
chr4	100706634	100706916	-	3046-	1.55601072	1.34055942	-0.000979624	NA	NA	NA	negative	negative
chr4	103956384	103956713	-	3215-	2.99481611	2.69555303	1.342116548	NA	NA	NA	Mueller + HC	Interneurons
chr4	130912296	130912598	-	3024-/Intergenic4	3.09691086	3.01884932	1.965822194	NA	NA	NA	HC + Amacrine cells	Interneurons
chr4	40994591	40995016	-	3326-/Aqp7-Intra	2.09420918	2.58195659	0.293942264	NA	NA	NA	Amacrine cells + HC + Mueller	Interneurons
chr6	127582881	127583163	-	3009-	1.61731687	0.31911029	-0.614659127	NA	NA	NA	negative	negative
chr6	48361745	48362148	+	3149+	3.93440563	3.79679328	1.521460404	NA	NA	NA	Amacrine cells	Interneurons
chr9	31656883	31657191	-	3259-	2.75159521	2.79424503	1.151503338	NA	NA	NA	Amacrine cells + Photoreceptors	Interneurons
chr9	50142608	50142868	+	3260+	1.48726742	2.2763465	-0.191911937	NA	NA	NA	HC	Interneurons

Supplementary Table 2: Table of individually tested enhancers and their activity pattern in the whole retina and log2 activity in csPRA. Second last column shows in which cell types GFP signal was detected under the microscope when single CREs were tested. 'negative' means no GFP signal could be found. The last column shows in which cell type CREs are expected to be active in csPRA. 'negative' means that activity is below threshold in csPRA.

Sequences of mutated CREs:

>107_WT
GAGGCTTTCACTGACCTTTCCATGTACGAGACTAGCCCCGCCCAGAGTGCTGTCTGGGATTAACTGTTACAGTCT
TAATTGTATTAGTATTTAGGTGACTTTGGGATTATTAGACTATTCCTGTGCATAGCTGCCTCTTGAGGGGAGAGC
CGGGAGAGAGAAGCAGCTGCATGTGCTGTGAGTAGGACATCTGGGGGCATCACTTTACCATCTCATAGTTCTA
GGGCCCTTGAAAACCTGGTATTGTCATGCTGGAAGGGT
>107_all_MEIS1_mut
GAGGCTTTCACTGACCTTTCCATGTACGAGACTAGCCCCGCCCAGAGTGCTGTCTGGGATTAACTGTTACAGTCT
TAATTGTATTAGTATTTAGGTGACTTTGGGATTATTAGACTATTCCTGTGCATAGCTGCCTCTTGAGGGGAGAGC
CGGGAGAGAGAAGCAGCTGCATGTGCTGTGAGTAGGACATCTGGGGGCATCACTTTACCATCTCATAGTTCTA
GGGCCCTTGAAAACCTGGTTTCTAGTTGCTGGAAGGGT
>107_all_SP1_mut
GAGGCTTTCACTGACCTTTCCATGTACGAGACTAAGGTAGTACAGAGTGCTGTCTGGGATTAACTGTTACAGTC
TTAATTGTATTAGTATTTAGGTGACTTTGGGATTATTAGACTATTCCTGTGCATAGCTGCCTCTTGAGGGGAGAG
CCGGGAGAGAGAAGCAGCTGCATGTGCTGTGAGTAGGACATCTGGGGGCATCACTTTACCATCTCATAGTTCT
AGGGCCCTTGAAAACCTGGTATTGTCATGCTGGAAGGGT
>107_all_ID4_mut
GAGGCTTTCACTGACCTTTCCATGTACGAGACTAGCCCCGCCCAGAGTGCTGTCTGGGATTAACTGTTCAGTCTT
AATTGTATTAGTATTTAGGTGACTTTGGGATTATTAGACTATTCCTGTGCATAGCTGCCTCTTGAGGGGAGAGCC
GGGAGAGAGACGCGATAGCATGTGCTGTGAGTAGGACATCTGGGGGCATCACTTTACCATCTCATAGTTCTAG
GGCCCTTGAAAACCTGGTATTGTCATGCTGGAAGGGT
>107_all_Nr1h3_mut
GAGGCTTTCATTACAATTTCCATGTACGAGACTAGCCCCGCCCAGAGTGCTGTCTGGGATTAACTGTTACAGTCT
TAATTGTATTAGTATTTAGGTGACTTTGGGATTATTAGACTATTCCTGTGCATAGCTGCCTCTTGAGGGGAGAGC
CGGGAGAGAGAAGCAGCTGCATGTGCTGTGAGTAGGACATCTGGGGGCATCACTTTACCATCTCATAGTTCTA
GGGCCCTTGAAAACCTGGTATTGTCATGCTGGAAGGGT
>483_WT
CGGGGCAGGAGTGAGTCATTCACACAGAGGCGGGTCAGAGAGTAGTGGTCACTCTTCAGCTTACAGCTCTCTC
TAGTCCTCTATCCAGACTCTAGTTTCATGAACTTTGTAGTTAGACATTTTTCCTAGTGAATATTTATTACCCCCCAC
TGTAATCCTTCATTTAACATAATATAAAATTTGTGGAAAGGGAGAGTAATTAGTAATAAATCATCATCTCATCCA
TTAGCAGTAAATAATGCCACTTTATCAAAGTCACAGCCATCGAACAGGCGGCTAGAGGTGGTTATGTATGCCAC
CCGACTGGAAGCAGGCCAAAAGCAAACCGCAGCCCCCGTTTATTATCCTAATTATGCCCTAATACGATGCCATC
TTTTTCTCCTATAAACTTGATGACAATAAAAGGGTAACAATGAAAATTGGCAGGGTAAGTGAGCAAGGAAGAT
AGGCTGGGAAACCACCTAGCCCCACCGGCTACCA
GCCTGAGTCCTGAGGCTGAAAGGGCTGAAAACCCCATGGGAATGAAATGGAGCAGGGGACTCAAGTGGTTGG
>483_all_MEIS1_mut
CGGGGCAGGAGTGAGTCATTCACACAGAGGCGGGTCAGAGAGTAGTGGTCACTCTTCAGCTTACAGCTCTCTC
TAGTCCTCTATCCAGACTCTAGTTTCATGAACTTTGTAGTTAGACATTTTTCCTAGTGAATATTTATTACCCCCCAC
TGTTCTAGTTCATTTAACATAATATAAAATTTGTGGAAAGGGAGAGTAATTAGTAATAAATCATCATCTCATCCA
TTAGCAGTAAATAATGCCACTTTATCAAAGTCACAGCCATCGAACAGGCGGCTAGAGGTGGTTATGTATGCCAC
CCGACTGGAAGCAGGCCAAAAGCAAACCGCAGCCCCCGTTTATTATCCTAATTATGCCCTAATACGATGCCATC
TTTTTCTCCTATAAACTTGATGACAATAAAAGGGTAACAATGAAAATTGGCAGGGTAAGTGAGCAAGGAAGAT
AGGCTGGGAAACCACCTAGCCCCACCGGCTACCA
GCCTGAGTCCTGAGGCTGAAAGGGCTGAAAACCCCATGGGAATGAAATGGAGCAGGGGACTCAAGTGGTTGG
>483_all_CRX_mut
CGGGGCAGGAGTGAGTCATTCACACAGAGGCGGGTCAGAGAGTAGTGGTCACTCTTCAGCTTACAGCTCTCTC
TAGTCCTCTATCCAGACTCTAGTTTCATGAACTTTGTAGTTAGACATTTTTCCTAGTGAATATTTATTACCCCCCAC
TGTAATCCTTCATTTAACATAATATAAAATTTGTGGAAAGGGAGAGTAATTAGTAATAAATCATCATCTCATCCA
TTAGCAGTAAATAATGCCACTTTATCAAAGTCACAGCCATCGAACAGGCGGCTAGAGGTGGTTATGTATGCCAC
CCGACTGGAAGCAGGCCAAAAGCAAACCGCAGCCCCCGTTTATTATCCTAATTATGCCCTAATACGATGCCATC
TTTTTCTCCTATAAACTTGCAGGTGTTAAAAGGGTAACAATGAAAATTGGCAGGGTAAGTGAGCAAGGAAGAT
AGGCTGGGAAACCACCTAGCCCCACCGGCTACCA
GCCTGAGTCCTGAGGCTGAAAGGGCTGAAAACCCCATGGGAATGAAATGGAGCAGGGGACTCAAGTGGTTGG
>483_all_NRL_mut

CGGGGCAGGAGTGAGTCATTCACACAGAGGCGGGTCAGAGAGTAGTGGTCACTCTTCAGCTTACAGCTCTCTC
TAGTCCTCTATCCAGACTCTAGTTTCATGAACTTTGTAGTTAGACATTTTTCCTAGTGAATATTTATTACCCCCCAC
TGTAAGCGAACGTAGAACATAATATAAAATTTGTGGAAAGGGAGAGTAATTAGTAATAAATCATCATCTCATCC
ATTAGCAGTAAATAATGCCACTTTATCAAAGTCACAGCCATCGAACAGGCGGCTAGAGGTGGTTATGTATGCCA
CCCGACTGGAAGCAGGCCAAAAGCAAACCGCAGCCCCCGTTTATTATCCTAATTATGCCCTAATACGATGCCAT
CTTTTTCTCCTATAAACTTGATGACAATAAAAGGGTAACAATGAAAATTGGCAGGGTAAGTGAGCAAGGAAGA
TAGGCTGGGAAACCACCTAGCCCCACCGGCTACCA
GCCTGAGTCCTGAGGCTGAAAGGGCTGAAAACCCCATGGGAATGAAATGGAGCAGGGGACTCAAGTGGTTGG
>483_all_En2_mut
CGGGGCAGGAGTGAGTCATTCACACAGAGGCGGGTCAGAGAGTAGTGGTCACTCTTCAGCTTACAGCTCTCTC
TAGTCCTCTATCCAGACTCTAGTTTCATGAACTTTGTAGTTAGACATTTTTCCTAGTGAATATTTATTACCCCCCAC
TGTAATCCTTCATTTAACATAATATAAAATTTGTGGAAAGGGAGAGCGGAGTAAACTAAATCATCATCTCATCCA
TTAGCAGTAAATAATGCCACTTTATCAAAGTCACAGCCATCGAACAGGCGGCTAGAGGTGGTTATGTATGCCAC
CCGACTGGAAGCAGGCCAAAAGCAAACCGCAGCCCCCGTTTATTATCCCGGAGTAAACCTAATACGATGCCATC
TTTTTCTCCTATAAACTTGATGACAATAAAAGGGTAACAATGAAAATTGGCAGGGTAAGTGAGCAAGGAAGAT
AGGCTGGGAAACCACCTAGCCCCACCGGCTACCA
GCCTGAGTCCTGAGGCTGAAAGGGCTGAAAACCCCATGGGAATGAAATGGAGCAGGGGACTCAAGTGGTTGG

Primers used for csPRA library preparation:

Name	Sequence
Primer #1	AATGATACGGCGACCACCGAGATCTACACTCTTTCCCTACACGACGCTCTTCCGATCT
Primer #2	AATGATACGGCGACCACCGAGATCTACACTCTTTCCCTACACGACGCTCTTCCGATCTTCCACTGGGAGAAGAGGAAGTCAAA

Indexing Primers:

Name	Sequence	Index
Primer #3	CAAGCAGAAGACGGCATACGAGATCGTGATGTGACTGGAGTTCAGACGTGTGCTCTTCCGATCT	1
Primer #4	CAAGCAGAAGACGGCATACGAGATACATCGGTGACTGGAGTTCAGACGTGTGCTCTTCCGATCT	2
Primer #5	CAAGCAGAAGACGGCATACGAGATATTGGCGTGACTGGAGTTCAGACGTGTGCTCTTCCGATCT	6
Primer #6	CAAGCAGAAGACGGCATACGAGATTACAAGGTGACTGGAGTTCAGACGTGTGCTCTTCCGATCT	12
Primer #7	CAAGCAGAAGACGGCATACGAGATTGGTCAGTGACTGGAGTTCAGACGTGTGCTCTTCCGATCT	4
Primer #8	CAAGCAGAAGACGGCATACGAGATGATCTGGTGACTGGAGTTCAGACGTGTGCTCTTCCGATCT	7
Primer #9	CAAGCAGAAGACGGCATACGAGATGACTGTGTGACTGGAGTTCAGACGTGTGCTCTTCCGATCT	5
Primer #10	CAAGCAGAAGACGGCATACGAGATTCAAGTGTGACTGGAGTTCAGACGTGTGCTCTTCCGATCT	8
Primer #11	CAAGCAGAAGACGGCATACGAGATGTGATCGTGACTGGAGTTCAGACGTGTGCTCTTCCGATCT	9

References:

1. Siegert, S. *et al.* Genetic address book for retinal cell types. *Nat. Neurosci.* **12,** 1197–1204 (2009).
2. Siegert, S. *et al.* Transcriptional code and disease map for adult retinal cell types. *Nat. Neurosci.* **15,** 487–95, S1-2 (2012).
3. Mo, A. *et al.* Epigenomic landscapes of retinal rods and cones. *Elife* **5,** 1–29 (2016).
4. Mo, A. *et al.* Epigenomic Signatures of Neuronal Diversity in the Mammalian Brain. *Neuron* **86,** 1369–1384 (2015).